Journal of Clinical and Translational Hepatology **2024** vol. 12(6) | 539–550
DOI: 10.14218/JCTH.2023.00562

Original Article

Mitochondrial GRIM19 Loss Induces Liver Fibrosis through NLRP3/IL33 Activation via Reactive Oxygen Species/NF-κB Signaling

Xiaohui Xu[1,2#], Jinmei Feng[1,3#], Xin Wang[4], Xin Zeng[5], Ying Luo[1], Xinyu He[1], Meihua Yang[6], Tiewei Lv[2], Zijuan Feng[1], Liming Bao[7], Li Zhao[1], Daochao Huang[1] and Yi Huang[2,8*]

[1]Institute of Pediatrics, Children's Hospital of Chongqing Medical University, National Clinical Research Center for Child Health and Disorders, Ministry of Education Key Laboratory of Child Development and Disorders, Chongqing Key Laboratory of Pediatric Metabolism and Inflammatory Diseases, Chongqing, China; [2]Department of Cardiology, Children's Hospital of Chongqing Medical University, National Clinical Research Center for Child Health and Disorders, Ministry of Education Key Laboratory of Child Development and Disorders, National Clinical Key Cardiovascular Specialty, Laboratory of Children's Important Organ Development and Diseases of Chongqing Municipal Health Commission, Chongqing, China; [3]Department of Laboratory Medicine, Chongqing Western Hospital, Chongqing, China; [4]Key Laboratory of Molecular Biology for Infectious Diseases, Ministry of Education, Institute for Viral Hepatitis, Chongqing Medical University, Chongqing, China; [5]Department of Laboratory Medicine, The Third People's Hospital of Chengdu, Chengdu, Sichuan, China; [6]Departments of Neurology, Epilepsy Center, Barnes-Jewish Hospital and Washington University School of Medicine, St. Louis, MO, USA; [7]Department of Clinical Pathology and Laboratory Medicine, Weill Cornell Medical College of Cornell University, New York, NY, USA; [8]Departments of Medicine (Oncology), Washington University School of Medicine, St. Louis, MO, USA

Received: December 21, 2023 | **Revised:** April 24, 2024 | **Accepted:** May 11, 2024 | **Published online:** May 28, 2024

Abstract

Background and Aims: Hepatic fibrosis (HF) is a critical step in the progression of hepatocellular carcinoma (HCC). Gene associated with retinoid-IFN-induced mortality 19 (GRIM19), an essential component of mitochondrial respiratory chain complex I, is frequently attenuated in various human cancers, including HCC. Here, we aimed to investigate the potential relationship and underlying mechanism between GRIM19 loss and HF pathogenesis. ***Methods:*** GRIM19 expression was evaluated in normal liver tissues, hepatitis, hepatic cirrhosis, and HCC using human liver disease spectrum tissue microarrays. We studied hepatocyte-specific *GRIM19* knockout mice and clustered regularly interspaced short palindromic repeats (CRISPR)/CRISPR-associated protein-9 (Cas9) lentivirus-mediated *GRIM19* gene-editing in murine hepatocyte AML12 cells *in vitro* and *in vivo*. We performed flow cytometry, immunofluorescence, immunohistochemistry, western blotting, and pharmacological intervention to uncover the potential mechanisms underlying GRIM19 loss-induced HF. ***Results:*** Mitochondrial GRIM19 was progressively downregulated in chronic liver disease tissues, including hepatitis, cirrhosis, and HCC tissues. Hepatocyte-specific *GRIM19* heterozygous deletion induced spontaneous hepatitis and subsequent liver fibrogenesis in mice. In addition, GRIM19 loss caused chronic liver injury through reactive oxygen species (ROS)-mediated oxidative stress, resulting in aberrant NF-κB activation via an IKK/IκB partner in hepatocytes. Furthermore, GRIM19 loss activated NLRP3-mediated IL33 signaling via the ROS/NF-κB pathway in hepatocytes. Intraperitoneal administration of the NLRP3 inhibitor MCC950 dramatically alleviated GRIM19 loss-driven HF *in vivo*. ***Conclusions:*** The mitochondrial GRIM19 loss facilitates liver fibrosis through NLRP3/IL33 activation via ROS/NF-κB signaling, providing potential therapeutic approaches for earlier HF prevention.

Citation of this article: Xu X, Feng J, Wang X, Zeng X, Luo Y, He X, *et al*. Mitochondrial GRIM19 Loss Induces Liver Fibrosis through NLRP3/IL33 Activation via Reactive Oxygen Species/NF-κB Signaling. J Clin Transl Hepatol 2024;12(6):539–550. doi: 10.14218/JCTH.2023.00562.

Introduction

Liver cancer is widely prevalent and ranks as the leading cause of cancer mortality in the digestive system worldwide.[1] Hepatic fibrosis (HF), an essential pathological stage in chronic liver disease, is critical to the progression of hepatocellular carcinoma (HCC), developing from early inflammation to cirrhosis and then to liver cancer.[2,3] Although significant advancements have been made in understanding the pathophysiological mechanism of liver fibrosis,[4–7] there is currently no effective strategy to reverse the end stage of HF, apart from liver transplantation. Therefore, identifying new therapeutic targets and understanding their underlying mechanisms of action are critical to developing novel strate-

Keywords: Liver fibrosis; GRIM19; Reactive Oxygen Species; NF-κB; NLRP3 inflammasome; IL33.

[#]Contributed equally to this work.

[*]**Correspondence to:** Yi Huang, Children's Hospital of Chongqing Medical University, No.136 Zhongshan Erd Road, Yuzhong District, Chongqing 400014, China. ORCID: https://orcid.org/0000-0002-8379-9684. Tel/Fax: +86-23-63622754, E-mail: yihuang828@foxmail.com

gies to prevent or delay liver fibrogenesis.

Liver fibrosis is characterized by the activation and proliferation of hepatic stellate cells (HSCs) and subsequent extracellular matrix (ECM) accumulation due to persistent hepatocellular injury and inflammatory stimulation.[8] Hepatocyte damage induced by various stimuli forms the initial stage of pathogenesis, contributing to inflammatory cell recruitment and cytokine secretion,[9] activating the transition of HSCs into myofibroblasts that produce collagen fibers, resulting in excessive ECM deposition.[3,5,9] However, most previous reports focus on the central role of HSCs and/or Kupffer cells in experimental HF models and human liver injuries.[4,5,7,10] Few studies have examined hepatocytes, which are frequently damaged in chronic liver injuries, although they are not typically regarded as the primary effector cells responsible for HF progression.[11,12] Hence, it is extremely important to explore the specific molecular interactions and underlying mechanisms in damaged liver cells for early HF prevention.

Mitochondrial dysfunction is a hallmark of liver fibrosis due to its frequent occurrence in various chronic liver diseases.[13,14] Increasing evidence shows that mitochondrial disorders are associated with HF development primarily through oxidative stress damage to hepatocytes induced by excessive ROS.[6,11–13] This emphasizes the need to pay more attention to mitochondrial homeostasis in hepatocytes during HF pathogenesis. However, there is limited characterization of the mechanisms protecting hepatocytes from mitochondrial damage in liver fibrogenesis.

The gene associated with retinoid-IFN-induced mortality 19 (GRIM19), also known as NDUFA13, a vital component of the mitochondrial respiratory chain (MRC) complex I,[15] has been reported to be inhibited in numerous human cancers, including gastric cancer and HCC,[15–17] indicating its potential role as a tumor suppressor. Our previous findings revealed a progressive downregulation of GRIM19 in chronic atrophic gastritis tissues, a precancerous lesion of gastric cancer, suggesting a crucial role of GRIM19 loss in inflammatory diseases and their premalignant progression.[16–18] However, whether GRIM19 loss is involved in liver fibrogenesis remains largely unknown. This study aimed to investigate the potential relationship between GRIM19 loss and HF pathogenesis and to explore underlying mechanisms *in vitro* and *in vivo*.

Methods

Human liver disease spectrum tissue microarrays (TMA)

Liver TMA slides containing 104 samples, including normal liver tissues (n=16), hepatitis (n=24), hepatic cirrhosis (n=32), and HCC (n=32), were commercially purchased from US Biomax, Inc (Cat. LV20812, corresponding clinical information and ethical materials were included). All samples were correctly labeled clinically and pathologically. The TMA slide was stained using IHC staining and scored as previously described.[16–18]

Cells, tissue culture, and reagents

Murine hepatocyte cells AML12 (Procell, Wuhan, China) were maintained in DMEM/F12 medium supplemented with 10% FBS (Gibco, Gaithersburg, MD, USA), 1× insulin-transferrin-selenium media supplement (Procell, Wuhan, China), 40 ng/mL dexamethasone (Procell, Wuhan, China), streptomycin (100 ug/mL), and penicillin (100 U/mL) at 37°C in a humidified 5% CO_2 atmosphere. The ROS scavenger N-acetylcysteine (NAC), NF-κB inhibitor PDTC, and Caspase1 inhibitor VX765 were obtained from AbMole Bioscience (Houston, TX, USA). The NLRP3 inhibitor MCC950 was from MCE (Houston, TX, USA). All chemical reagents were commercially obtained from Sigma-Aldrich (St Louis, MO, USA) unless otherwise indicated. All antibodies used in this study are provided in Supplementary Table 1.

GRIM19 gene-editing mediated by CRISPR/Cas9 lentivirus

CRISPR/Cas9-mediated recombinant lentivirus carrying specific small-guide RNA targeting *GRIM19* at position 11656 (sgRNA-56), 11657 (sgRNA-57), and 11658 (sgRNA-58), as well as the corresponding negative control (NC), were commercially constructed with a GFP reporter gene by GeneChem Co (Shanghai, China). AML12 cells were infected by CRISPR/Cas9 recombinant lentivirus with a multiplicity of infection of 30–50, and GFP-positive cells were sorted by flow cytometry (FACS Aria II, BD) to establish single-cell clones following established protocols.[17] Western blotting and immunofluorescence (IF) staining were performed to determine GRIM19 expression.

Transgenic mice model and pharmacological intervention in vivo

GRIM19 conditional knockout (CKO) mice *GRIM19*$^{flox/flox}$ (*GRIM19*$^{fl/fl}$) with the exon 3 of *GRIM19* flanked by loxP (C57BL/6J X129/Sv background) were commercially obtained from Cyagen Bio Inc (Suzhou, China) as previously described.[18–20] Alb-Cre transgenic mice [(B6.Cg-Tg(Alb-cre)21Mgn/J, JAX-003574)] were purchased from the Shanghai Biomodel Organism Center (Shanghai, China). Hepatocyte-specific *GRIM19* knockout (KO) mice were acquired by crossing *GRIM19*$^{fl/fl}$ and Alb-Cre transgenic mice. DNAs from tail or liver tissues were subjected to PCR genotyping, while *GRIM19* expression was confirmed by Western blotting and IF. *GRIM19* heterozygous KO mice (*GRIM19*$^{fl/-}$/Alb-Cre, named *GRIM19*$^{fl/-}$) were used in this study, and *GRIM19*$^{fl/fl}$ mice were littermate controls. For experimental intervention in mice, *GRIM19*$^{fl/-}$ mice (eight to nine months) were randomly divided into two groups (n=8 mice/group) and administrated with either PBS control or MCC950 (10 mg/kg in PBS) via intraperitoneal (i.p.) injection three times per week for four consecutive weeks. Animals were kept, housed, and bred under specific pathogen-free conditions as previously described.[16–20] All procedures were reviewed and approved by the Institutional Animal Care and Use Committee of Chongqing Medical University (CHCMU-IACUC20210114023).

Histology and Immunohistochemistry (IHC)

Histology and IHC staining were performed as previously described.[16–18] Liver tissues were fixed in 10% buffered formalin for 48 h, dehydrated in various ethanol concentrations, and embedded in paraffin for preparing histopathological analysis. Tissue sections (4 μm) underwent H&E staining and Masson's trichrome staining (Solarbio, Beijing, China) in accordance with the manufacturer's instructions. The fibrosis stage in the liver was evaluated based on the Ishak score. IHC staining was conducted utilizing Elivision plus Polymer HRP IHC Kit (Maixin, Fujian, China) and DAB Kit (ZSGB-Bio, Beijing, China). The number of positive cells and staining intensity were evaluated to determine the IHC score, as previously specified.[16–18]

Immunofluorescence (IF) staining

IF staining was performed on paraffin-embedded tissue sections (4 μm) or fresh frozen liver tissues (8 μm) as described

previously.[17–20] Briefly, normal goat serum (Solarbio, Beijing, China) was used to block tissue sections for 1 h at room temperature. Primary antibodies were incubated overnight at 4°C, followed by AF488, AF555, or AF647-conjugated secondary antibody (Bioss, Beijing, China) according to the manufacturer's instructions at room temperature. 4′,6-diamidino-2-phenylindole (DAPI) was used to stain the nuclei. Images were acquired by the laser confocal microscope (A1R, Nikon, Japan), and mean fluorescent intensity (MFI) was quantified using NIS-Element 5.20 Software.

Intracellular ROS and mitochondrial ROS (mROS) measurements

Intracellular ROS and mROS in cells or fresh frozen tissue sections (8 μm) were measured using 10 μM Dihydroethidium (DHE) (Sigma, USA) or 5 μM MitoSOX Red (Thermo Fisher Scientific, Waltham, USA) by flow cytometry or IF staining as described previously.[17,18] Indicated cells were resuspended, and MFI was measured by flow cytometry on a FACS Calibur flow cytometer (BD Bioscience), with data analyzed using FlowJo software (TreeStar, Ashland, OR). DAPI was used to stain the nuclei. Images were obtained using the laser confocal microscope (A1R, Nikon, Japan), and MFI was quantified through NIS-Element 5.20 Software.

Intracellular adenosine triphosphate (ATP) level assay

Intracellular ATP levels were measured using an ATP Assay Kit (Beyotime Biotech, Haimen, China) following the manufacturer's instructions. AML12 cells (1.0×10^6) were homogenized and lysed in 200 μL of ice-cold lysis buffer, then centrifuged at 12,000 g for 5 m at 4°C. Relative Light Units were determined from the supernatant using a Synergy H1 microplate reader (Bio Tek, USA).

Intracellular reduced glutathione (GSH)/oxidized glutathione (GSSG) ratio and $NADP^+$/NADPH ratio analysis

The intracellular $NADP^+$/NADPH ratio and GSH/GSSG ratio were determined using the $NADP^+$/NADPH Assay Kit (Beyotime, Haimen, China) and GSH/GSSG Ratio Detection Assay Kit (Beyotime, Haimen, China), respectively. The oxidative status in AML12 cells was assessed using a Synergy H1 microplate reader (Bio Tek, CA, USA) according to the manufacturer's instructions as described previously.[17,18]

Western blotting

Protein extraction and western blotting were performed as described previously.[18–20] Liver tissues or AML12 cells were subjected to total protein extraction. Cellular components were prepared using NE-PER nuclear and cytoplasmic extraction reagents (Thermo Fisher Scientific, Waltham, USA). Protein extracts were quantified using an enhanced BCA Protein Assay Kit (Beyotime, Haimen, China). Samples (20–30 μg) were resolved by SDS-PAGE and transferred to polyvinylidene fluoride membranes (0.22 μM) (Roche, Mannheim, Germany). QuickBlock™ Blocking Buffer (Beyotime, Haimen, China) was applied to block the polyvinylidene fluoride membranes, followed by incubation with the indicated primary antibody overnight at 4°C. HRP-conjugated secondary antibodies were then incubated for 1–2 h at room temperature after washing with TBST buffer. Visualization was performed using a WesternBright ECL kit (Advansta, Menlo Park, CA, USA) on a ChemiDoc™Touch Imaging System (Bio-Rad, Hercules, CA, USA). Total protein levels were normalized using β-actin as a loading control.

Flow cytometry

Flow cytometry was performed on a FACS Calibur flow cytometer (BD Bioscience), and the data were analyzed using FlowJo software (Tree Star, Ashland, OR) as described previously.[17,18] GFP-positive AML12 cells were sorted after transfection.

Statistical analysis

Statistical analysis was performed using GraphPad Prism 8.0 (GraphPad, San Diego, CA) as previously described.[17,18] All data were expressed as the mean±SD unless otherwise specified. An unpaired Student's *t-test* (two groups) or a one-way analysis of variance (more than two groups) was applied to analyze statistical differences. A *p*-value of $p<0.05$ was considered statistically significant.

Results

GRIM19 is downregulated in human chronic liver fibrosis tissues

GRIM19 was identified as frequently reduced in various human cancers, including HCC.[15–17,21] To investigate whether GRIM19 loss is associated with liver fibrogenesis, we evaluated GRIM19 protein levels in tissues from patients with chronic liver diseases using human liver disease spectrum TMAs containing normal liver, hepatitis, cirrhosis, and HCC tissues. As shown in Figure 1A, IHC staining revealed progressive downregulation of GRIM19 protein in hepatitis, cirrhosis, and HCC tissues compared with normal liver tissues. Furthermore, we observed that GRIM19 protein was predominantly distributed in the cytoplasm of normal liver tissues with dense dot-like or uniform patterns, whereas in hepatitis, cirrhosis, and HCC tissues, GRIM19 was clearly present perinuclearly or even in the nucleus with a dense dot distribution (Fig. 1B). These findings suggest that the downregulation of GRIM19 may correlate with the progression of chronic liver diseases.

Hepatocyte-specific GRIM19 heterozygous deletion is sufficient to trigger spontaneous liver fibrogenesis in mice

Given the downregulation of GRIM19 in chronic human liver diseases, we investigated whether GRIM19 loss is responsible for liver fibrogenesis. To this end, we generated a genetic hepatocyte-specific *GRIM19* KO mice model using the Cre-loxP-based system by crossing transgenic *GRIM19* CKO and Alb-Cre mice to obtain hepatocyte-specific heterozygous *GRIM19* deletion mice (Supplementary Fig. 1). H&E staining demonstrated that hepatocyte-specific *GRIM19* loss caused abnormal liver structure, sinusoidal destruction, and swollen hepatocytes compared with littermate controls (Fig. 2A). Interestingly, we did not observe obvious accumulation of extracellular collagen fibers in *GRIM19*-deleted liver tissues from four-week-old mice, as demonstrated by Masson staining (Fig. 2B). However, we observed a significant infiltration of $CD45^+$ and MPO^+ cells and a slight increase in $F4/80^+$ cells (Fig. 2C). Therefore, these findings suggest that hepatocyte-specific GRIM19 ablation triggers spontaneous hepatitis at an early stage.

To explore whether GRIM19 loss-induced hepatitis could progress to HF, we extended our observation of hepatocytes-specific *GRIM19* deletion mice to a period of two years. Similar to the results from four-week-old mice, H&E staining showed the presence of abnormal liver structures and damaged hepatocytes in two-year-old *GRIM19*-KO mice compared with littermate controls (Fig. 2D). However, as demonstrated

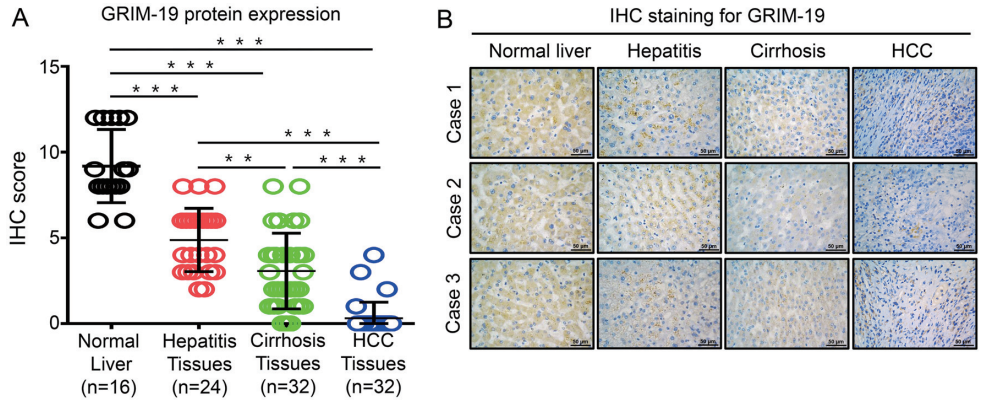

Fig. 1. GRIM19 (gene associated with retinoid-IFN-induced mortality 19) is downregulated in human chronic liver disease tissues. (A) GRIM19 expression was analyzed by immunohistochemistry (IHC) staining in liver disease spectrum tissue microarrays (TMAs) with normal liver, hepatitis, cirrhosis, and hepatocellular carcinoma (HCC) tissues. (B) The distribution of GRIM19 protein between normal liver and chronic liver disease tissues. Representative images from three different cases are shown. ***p*<0.01, ****p*<0.001 between the indicated two groups determined by unpaired student's *t*-test. Scale bars: 50 μm, Original magnification: ×400.

in Figure 2E with Masson staining, we observed the accumulation of extracellular collagen fibers in GRIM19-deficient livers, indicating that liver fibrogenesis from hepatitis progressed with age. We also observed significant infiltrations of $CD45^+$, MPO^+, and $F4/80^+$ cells (Fig. 2F). Tumor necrosis factor-α (TNFα) (Supplementary Fig. 2A, B) and TGFβ1 (Supplementary Fig. 2C, D) were significantly increased and co-localized with activated $F4/80^+$ cells in *GRIM19*-deleted liver tissues, indicating that macrophage-derived TNFα and TGFβ1 play a vital role in GRIM19 loss-induced liver fibrogenesis. Therefore, our data suggest that heterozygous *GRIM19* deletion induces persistent hepatitis and consequent HF with age.

Next, we further investigated HSC activation and the presence of fibrosis-associated proteins in liver tissues from two-year-old *GRIM19*-deficient mice. As shown in Figure 2G, GRIM19 ablation significantly increased both α-SMA and Desmin levels, indicating enhanced proliferation and activation of HSCs. Besides the fibrotic marker α-SMA, pro-fibrotic proteins Collagen I and TIMP1 demonstrated a marked increase (Fig. 2H, I), indicating an imbalance in ECM synthesis and degradation in *GRIM19*-deleted liver tissues. Moreover, we found that activated HSCs with normal GRIM19 expression (Supplementary Fig. 3A) were surrounded by higher levels of TGFβ1 and Collagen III (Supplementary Fig. 3B, C), indicating that macrophage-derived TGFβ1 may contribute to HSC activation. Together, these results suggest that hepatocyte-specific *GRIM19* deletion is sufficient to trigger spontaneous liver fibrogenesis in mice.

GRIM19 loss induces chronic liver injury by oxidative stress

To investigate the mechanism by which GRIM19 loss induces liver fibrogenesis *in vitro*, we used CRISPR/Cas9 sgRNA-mediated gene editing to knock down GRIM19 expression in the murine hepatocyte AML12 cell line (Supplementary Fig. 4A, B). Among three sgRNA targets, CRISPR/Cas9-mediated sgRNA-11658 (sgRNA-58) demonstrated the most effective inhibition of GRIM19 expression (Supplementary Fig. 4C). We then isolated stable GRIM19-deficient AML12 clones by FACS sorting (Supplementary Fig. 4D). Consequently, AML12 cells expressing sgRNA-58 (AML12-58 cells) or a negative control (NC) (AML12-NC cells) were used for subsequent analysis.

Next, we investigated the effect of GRIM19 loss on chronic liver injury, a critical initial event for liver fibrogenesis.[3,9] As shown in Figure 3A, B, we observed that GRIM19 loss markedly increased intracellular ROS and mROS, as well as 8-OHdG, a marker of ROS-induced DNA damage[18] *in vitro*. Furthermore, GRIM19 loss significantly decreased ATP content (Fig. 3C) and the GSH/GSSG ratio (Fig. 3D, left panel), while increasing the $NADP^+$/NADPH ratio (Fig. 3D, right panel) in AML12 cells, indicated that GRIM19 loss causes chronic hepatocyte injury via ROS-induced oxidative stress. In addition, we observed increased intracellular ROS (Fig. 3E), mROS production (Fig. 3F), and 8-OHdG levels (Fig. 3G) in GRIM19-deficient mice livers, indicating that GRIM19 plays an essential role in the homeostasis of oxidative stress in hepatocytes. Overall, these data suggest that GRIM19 loss exerts a crucial role in oxidative damage-induced hepatocyte injury.

GRIM19 loss induces ROS-dependent NF-κB activation in vitro and in vivo

NF-κB activation has been frequently involved in liver inflammation.[22] Given the dual role of ROS in oxidative damage and NF-κB signaling, we examined the effect of GRIM19 loss on NF-κB activation. We found that the expression of both p65 and its phosphorylated form, p-p65, was significantly enhanced after *GRIM19* knockdown *in vitro* (Fig. 4A). We also observed a clear increase in p-p65 levels, accompanied by a minor increase in p65 levels, *in vivo* (Fig. 4B). Furthermore, NF-κB-responsive targets including IL6, TNFα, VEGF, VCAM1, and ICAM1 were significantly increased both *in vivo* and *in vitro* (Fig. 4A, B). We discovered markedly altered NF-κB regulator proteins including p-IKKα/β, IKKα/β, p-IκB-α, and IκB-α (Fig. 4C), and also found that cytoplasmic and nuclear p65 levels were both increased after GRIM19 loss (Fig. 4D–F). In addition, NF-κB inhibitor PDTC significantly abrogated GRIM19 loss-induced p65 activation and downstream targets in AML12 cells (Fig. 4G). To further clarify the role of ROS in GRIM19 loss-induced NF-κB activation, NAC (a ROS scavenger) was applied to determine whether ROS suppression could inhibit GRIM19 loss-induced NF-κB activation. As shown in Figure 4H, I, NF-κB activation, its downstream targets, and the NF-κB regulator proteins normally promoted by GRIM19 loss were significantly attenuated after NAC intervention in AML12-58 cells. Hence, these results suggest that GRIM19 loss significantly activates NF-κB in a ROS-dependent manner.

GRIM19 loss-driven activation of the NLRP3 inflammasome is critical to liver fibrogenesis in mice

It has been shown that mROS facilitates liver fibrogenesis

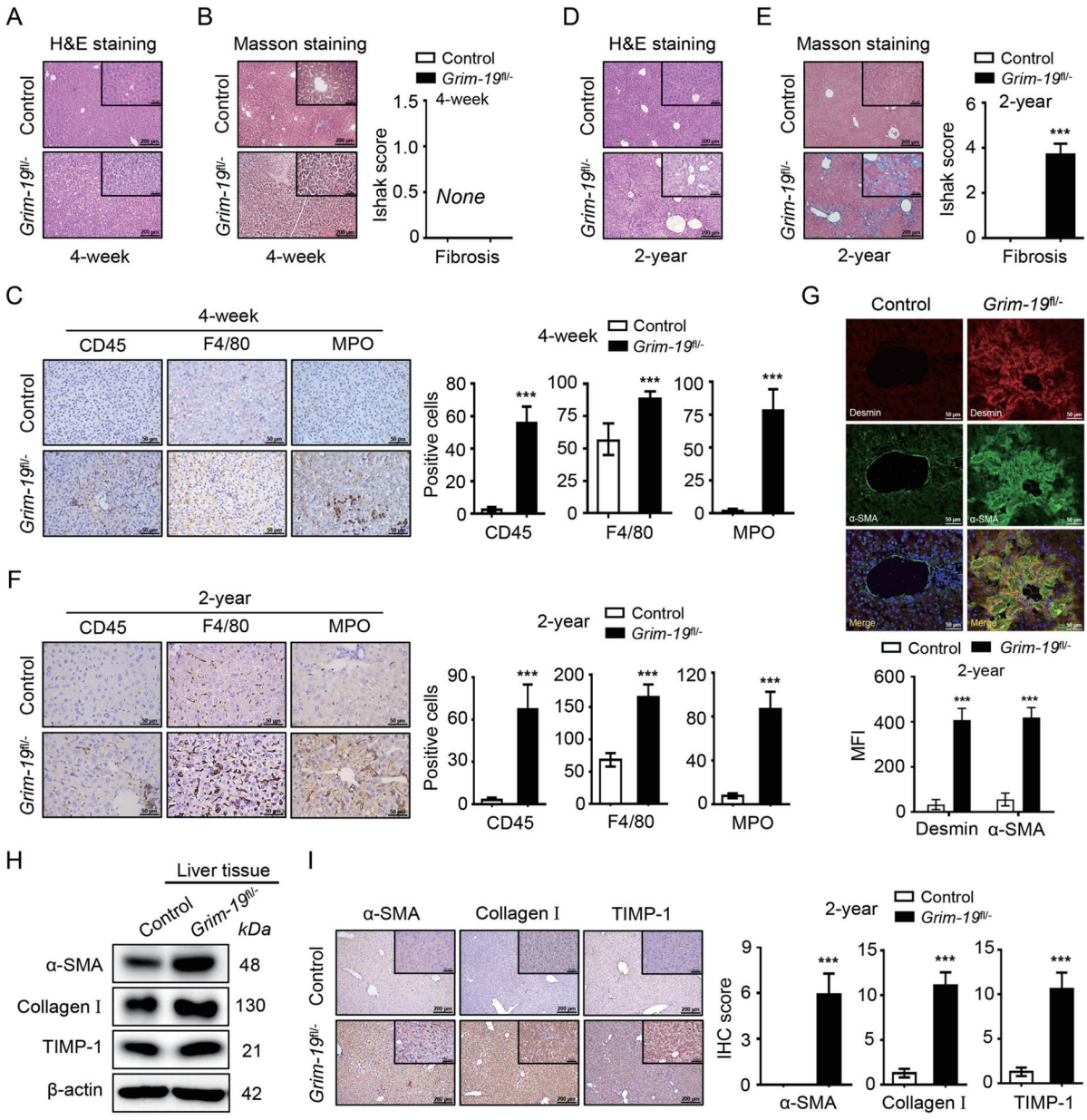

Fig. 2. Hepatocyte-specific *GRIM19* (gene associated with retinoid-IFN-induced mortality 19) deletion triggers spontaneous chronic liver fibrogenesis in mice. (A–B) Histological analysis of the liver tissues from littermate control *GRIM19*$^{fl/fl}$ mice (Control) and *GRIM19*-KO mice (*GRIM19*$^{fl/-}$) at four weeks of age. Hematoxylin and eosin (H&E) staining (A) and Masson trichrome staining (B) were performed to analyze histological changes and liver fibrosis, respectively. Ishak score was used to evaluate histological grading and staging for fibrosis. None: No fibrosis. (C) Immunohistochemistry (IHC) staining for immune cell markers CD45, F4/80, and MPO in liver tissues of control and *GRIM19*$^{fl/-}$ mice at four weeks of age. (D, E) Histological analysis of the liver tissues of control and *GRIM19*$^{fl/-}$ mice with two years of age. H&E staining (D) and Masson trichrome staining (E) were performed to detect histological alterations and liver fibrosis, respectively. Ishak score was used to evaluate histological grading and staging for fibrosis. (F) IHC staining for immune cell markers CD45, F4/80, and MPO in the liver tissues of control and *GRIM19*$^{fl/-}$ mice at two years of age. (G–I) Fibrosis-associated proteins in the liver tissues of control and *GRIM19*$^{fl/-}$ mice with two years of age. Dual immunofluorescence (IF) staining was used to analyze the co-expression of Desmin and α-SMA (G). Western blotting (H) and IHC staining (I) were performed to detect α-SMA, Collagen I and TIMP1 expression. β-actin was used as a loading control. DAPI was used to stain the nuclei. Mean fluorescent intensity (MFI) was used to quantify the expression of proteins in IF staining. Representative images are shown. Data are expressed as mean±SD. Scale bars: (main) 200 μm; (inset) 50 μm. ***p<0.001 between the indicated two groups determined by unpaired student's *t-test*. TIMP1, tissue inhibitor of metalloproteinase-1; MPO, myeloperoxidase; α-SMA, alpha-smooth muscle actin; DAPI, 4′,6-diamidino-2-phenylindole.

by activating the NLRP3 inflammasome,[23,24] which directly promotes liver fibrosis by activating Kupffer cells (KCs) and HSCs in mice.[25] Therefore, we investigated whether the NLRP3 inflammasome is involved in GRIM19 loss-driven liver fibrogenesis. Using hepatocyte-specific *GRIM19* KO mice, we observed a significant increase in NLRP3, ASC, and Caspase1 protein expression (Fig. 5A). Moreover, IL1β and IL33, two critical NLRP3-induced proinflammatory cytokines, were markedly elevated in GRIM19-deficient liver tissues as shown by western blotting (Fig. 5A), indicating aberrant NLRP3 ac-

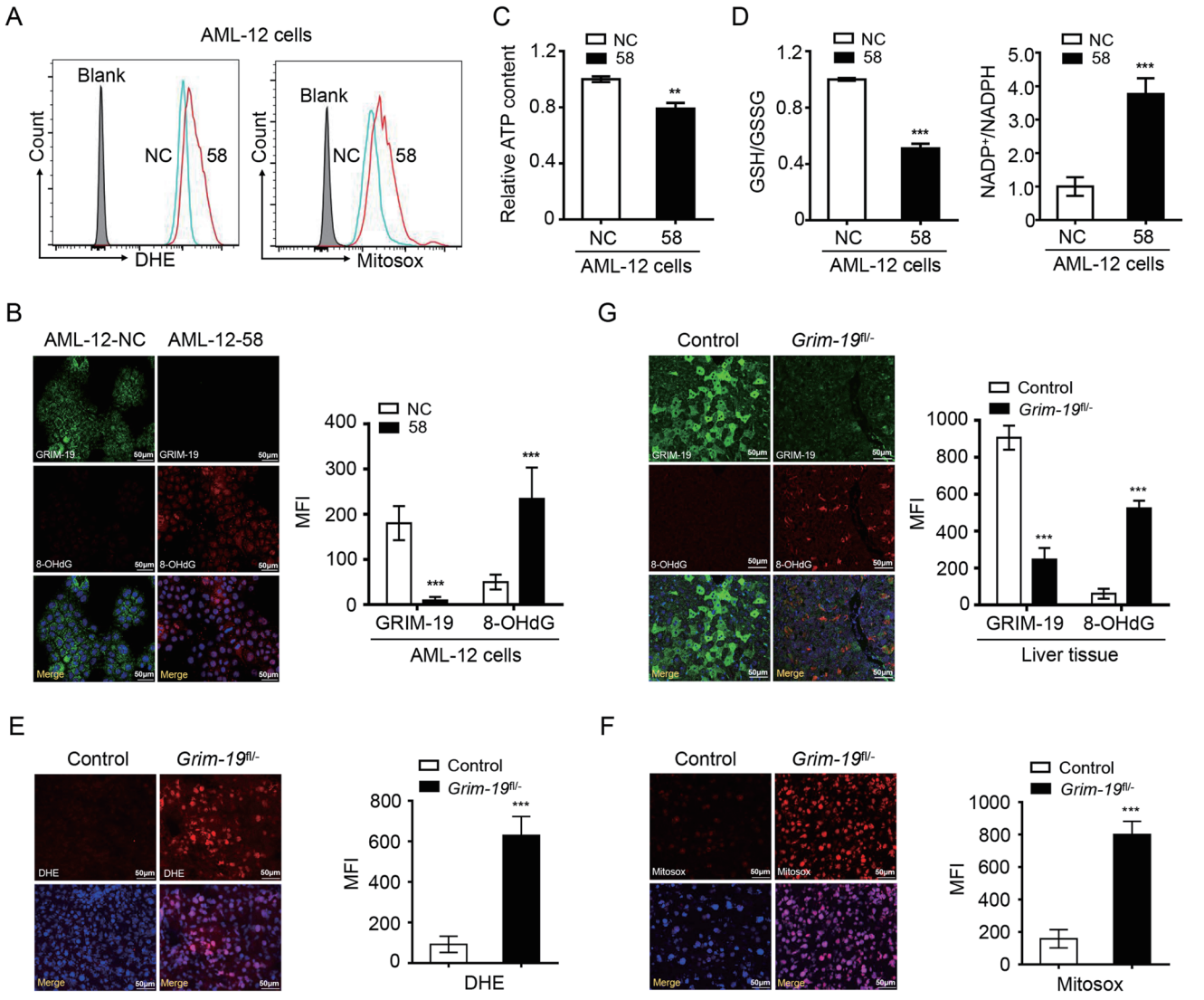

Fig. 3. GRIM19 (gene associated with retinoid-IFN-induced mortality 19) loss induces liver injury by reactive oxygen species (ROS)-induced oxidative stress. (A) GRIM19 loss induces abnormal ROS release *in vitro*. Intracellular ROS and mitochondrial ROS (mROS) were detected by flow cytometry in AML12 cells. (B–D) GRIM19 loss induces aberrant oxidative stress *in vitro*. DNA damage marker 8-oxodeoxyguanosine (8-OHdG) was detected by immunofluorescence (IF) staining in GRIM19-deficient AML12 cells (B). Oxidative stress was evaluated by analyzing intracellular ATP content (C), GSH/GSSG ratio, and NADP+/NADPH ratio (D) in GRIM19-deficient AML12 cells. (E, F) GRIM19 loss induces abnormal ROS release *in vivo*. Intracellular ROS (E) and mROS (F) were detected by IF staining in fresh frozen liver tissues from two-year-old mice. (G) GRIM19 loss causes oxidative damage *in vivo*. DNA damage 8-OHdG was determined by IF staining in fresh frozen liver tissues from two-year-old mice. Representative images are shown. DAPI was used to stain the nuclei. Mean fluorescent intensity (MFI) was used to quantify protein expression in IF staining. Data are expressed as mean±SD. Scale bar: 50 μm. $^{**}p<0.01$, $^{***}p<0.001$ between the indicated groups determined by unpaired student's *t-test*. AML-12, alpha mouse liver 12; NC, negative control; DAPI, 4′,6-diamidino-2-phenylindole.

tivation during liver fibrogenesis. Furthermore, dual IF staining revealed that the increased levels of NLRP3, IL33, and IL1β were mainly observed in hepatocytes (Fig. 5B) rather than HSCs (Supplementary Fig. 5) in KO mice. These findings indicate that hepatocyte-specific *GRIM19* deletion can directly trigger abnormal activation of the NLRP3 inflammasome.

To clarify the crucial role of NLRP3 activation in GRIM19 loss-induced liver fibrogenesis, we applied MCC950, an NLRP3 inhibitor, through intraperitoneal administration to analyze whether NLRP3 inhibition could alleviate the fibrotic liver phenotype in *GRIM19* KO mice (Supplementary Fig. 6A). We found that MCC950 treatment significantly decreased NLRP3 inflammasome activation and IL1β and IL33 levels in *GRIM19* KO mice (Fig. 5C–D). Furthermore, we also observed a decrease in GRIM19 loss-induced $CD45^+$, MPO^+ cells, and M2-type macrophages after MCC950 administration (Supplementary Fig. 6B, C, Supplementary Fig. 7). Interestingly, NLRP3 inhibition also attenuated GRIM19 loss-induced liver fibrosis, with reduced collagen deposition around the hepatic central vein (Fig. 5E) and decreased expression of α-SMA, fibrotic molecules Collagen I, and TIMP1 (Fig. 5F, G). These results suggest that NLRP3 activation is critical to GRIM19 loss-induced liver fibrogenesis in mice.

GRIM19 loss triggers aberrant NLRP3/IL33 activation through ROS/NF-κB signaling

Considering the increase in IL33 induced by NLRP3 in *GRIM19*

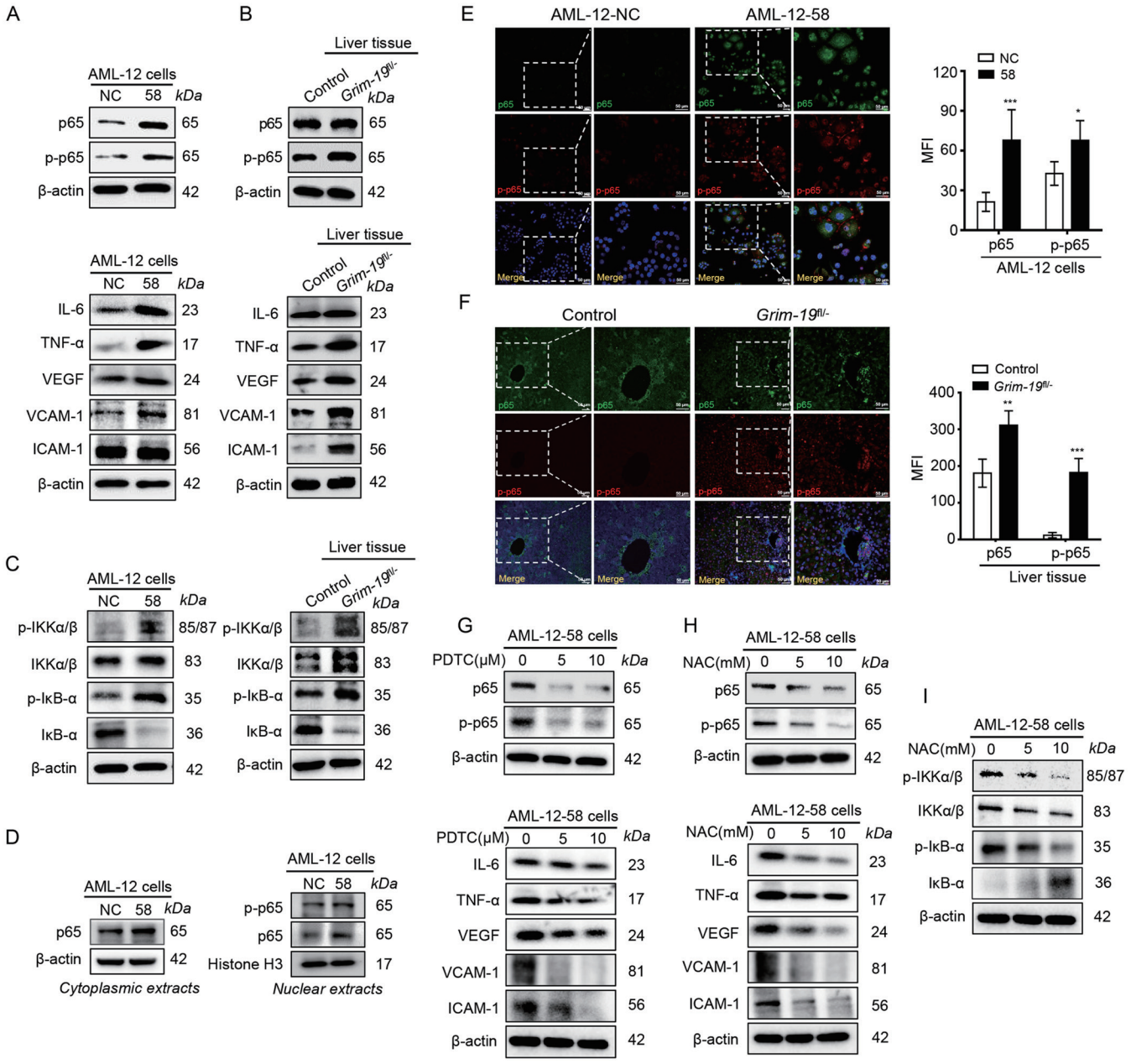

Fig. 4. GRIM19 (gene associated with retinoid-IFN-induced mortality 19) loss induces reactive oxygen species (ROS)-dependent NF-κB activation *in vitro* and *in vivo*. (A–F) GRIM19 loss promotes NF-κB/p65 activation *in vitro* and *in vivo*. Total p65, p-p65, and NF-κB downstream targets IL6, TNFα, VEGF, VCAM1, and ICAM1 were analyzed by western blotting in GRIM19-deficient AML12 cells (A) and liver tissues (B). NF-κB-regulatory proteins pIKKα/β, IKKα/β, pIκBα, and IκBα were detected by western blotting in GRIM19-deficient AML12 cells and liver tissues (C). NF-κB p65 levels in nuclear or cytoplasmic extractions were analyzed by western blotting in GRIM19-deficient AML12 cells (D). p65 and p-p65 co-expression was detected by dual immunofluorescence (IF) staining in GRIM19-deficient AML12 cells (E) and liver tissues (F). (G) NF-κB inhibition reverses GRIM19 loss-driven NF-κB/p65 activation *in vitro*. GRIM19-deficient AML12 cells were treated with NF-κB inhibitor PDTC (0, 5, 10 μM) for 16 h. The expression of p65, p-p65, and NF-κB downstream targets were determined by western blotting. (H, I) Reactive oxygen species (ROS) scavenger abrogates GRIM19 loss-driven NF-κB/p65 activation *in vitro*. GRIM19-deficient AML12 cells were treated with NAC (0, 5, 10 mM) for 16 h, then p65, p-p65, and NF-κB downstream targets were detected by western blotting (H). NF-κB-regulatory proteins pIKKα/β, IKKα/β, pIκBα, and IκBα were detected by western blotting in GRIM19-deficient AML12 cells after NAC treatment (0, 5, 10 mM) for 16 h (I). β-actin was used as a loading control. DAPI was used to stain the nuclei. Mean fluorescent intensity (MFI) was used to quantify the expression of proteins in IF staining. Data are expressed as mean±SD. Scale bars: 50 μm. *p<0.05, **p<0.01, ***p<0.001 between the indicated groups determined by unpaired student's *t-test*. AML-12, alpha mouse liver 12; NC, negative control; NAC, N-acetylcysteine; PDTC, ammonium pyrrolidinedithiocarbamate; IL-6, interleukin 6; VCAM-1, vascular cell adhesion molecule 1; ICAM-1, intercellular adhesion molecular 1; VEGF, vascular endothelial growth factor; TNF, tumour necrosis factor; DAPI, 4′,6-diamidino-2-phenylindole.

KO mice, we attempted to explore the regulatory pathway involved in NLRP3/IL33 activation, which may play a pivotal role in HF pathogenesis.[26] Consistent with our observations in liver tissues *in vivo*, we found considerably elevated levels of IL1β and IL33 in GRIM19-deficient AML12 cells (Fig. 6A, B). Therefore, we applied specific inhibitors to determine

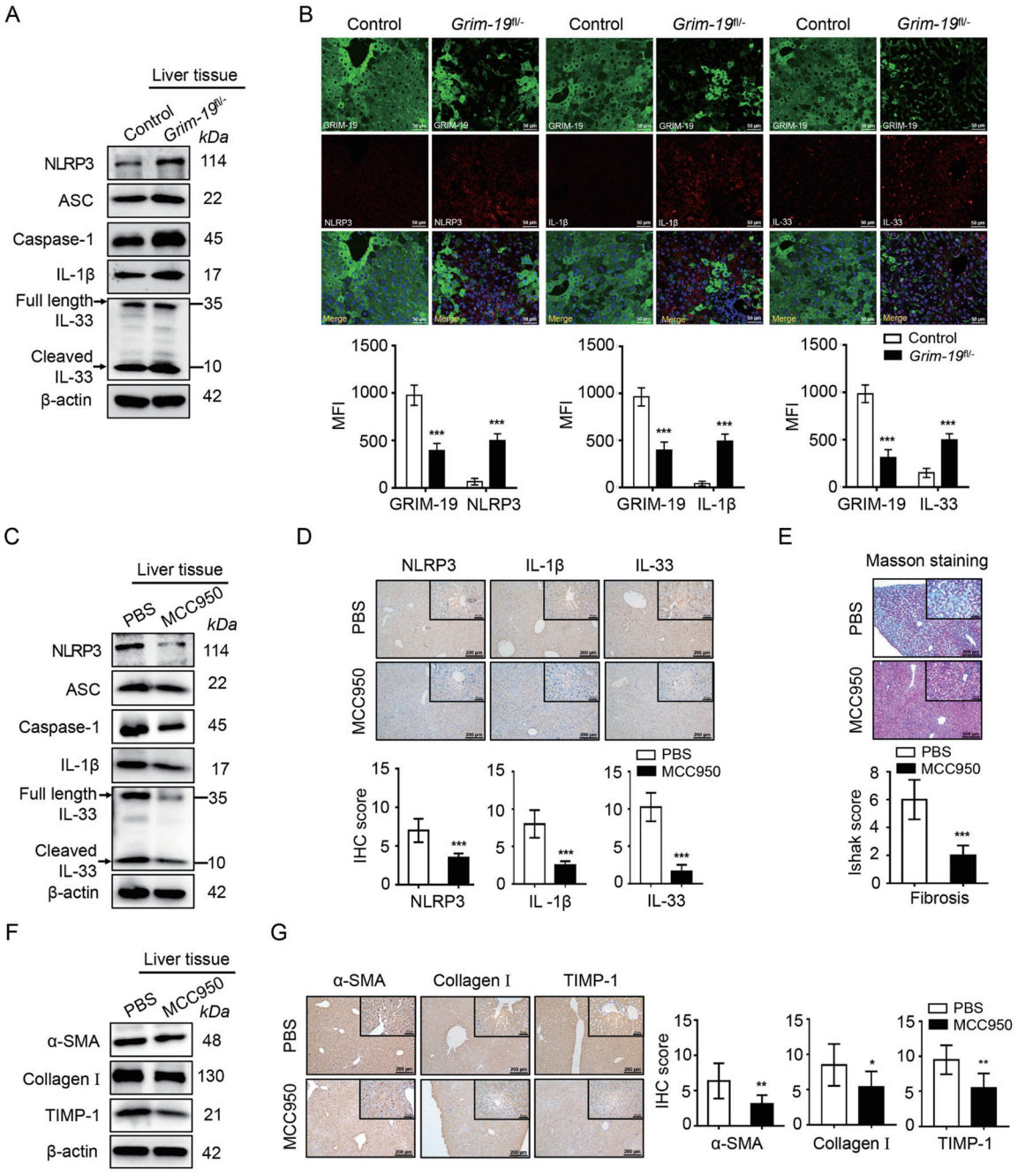

Fig. 5. GRIM19 (gene associated with retinoid-IFN-induced mortality 19) loss-driven NLRP3 inflammasome is critical for liver fibrogenesis in mice. (A, B) GRIM19 loss triggers NLRP3 inflammasome activation *in vivo*. Western blotting was used to detect NLRP3 inflammasome complex, as well as IL1β and IL33 cytokines in liver tissues (A). Dual immunofluorescence (IF) staining was used to detect GRIM19 & NLRP3, GRIM19 & IL1β, and GRIM19& IL33 in liver tissues (B). (C, D) MCC950 treatment attenuated GRIM19 loss-driven NLRP3 inflammasome activation *in vivo*. NLRP3 inflammasome, IL1β, and IL33 expression in liver tissues were detected by western blotting (C) or immunohistochemistry (IHC) staining (D). (E–G) MCC950 treatment alleviates GRIM19 loss-driven liver fibrogenesis *in vivo*. Masson trichrome staining was performed to analyze histological changes and liver fibrosis after MCC950 treatment, and the Ishak score was used to evaluate histological grading and staging for fibrosis (E). Fibrosis-associated proteins α-SMA, Collagen I, and TIMP1 in liver tissues were detected by western blotting (F) and IHC staining (G) after MCC950 treatment. β-actin was used as a loading control. DAPI was used to stain the nuclei. Mean fluorescent intensity (MFI) was used to quantify the expression of proteins in IF staining. Data are presented as mean±SD of three independent experiments. Representative images are shown. Scale bars: (main) 200 μm; (inset) 50 μm. *p<0.05, **p<0.01, ***p<0.001 between the indicated groups determined by unpaired student's t-test. α-SMA, alpha-smooth muscle actin; DAPI, 4′,6-diamidino-2-phenylindole; TIMP-1, Tissue inhibitor of metalloproteinase-1; IL, interleukin.

the exact roles of ROS and NF-κB in NLRP3/IL33 activation. We found that both NAC (ROS scavenger) and PDTC (NF-κB inhibitor) markedly diminished GRIM19 loss-driven NLRP3 inflammasome activation, as well as IL1β and IL33 expression (Fig. 6C, D). We also used MCC950 and VX765 (an inhibitor of Caspase1) to further investigate the role of the NLRP3

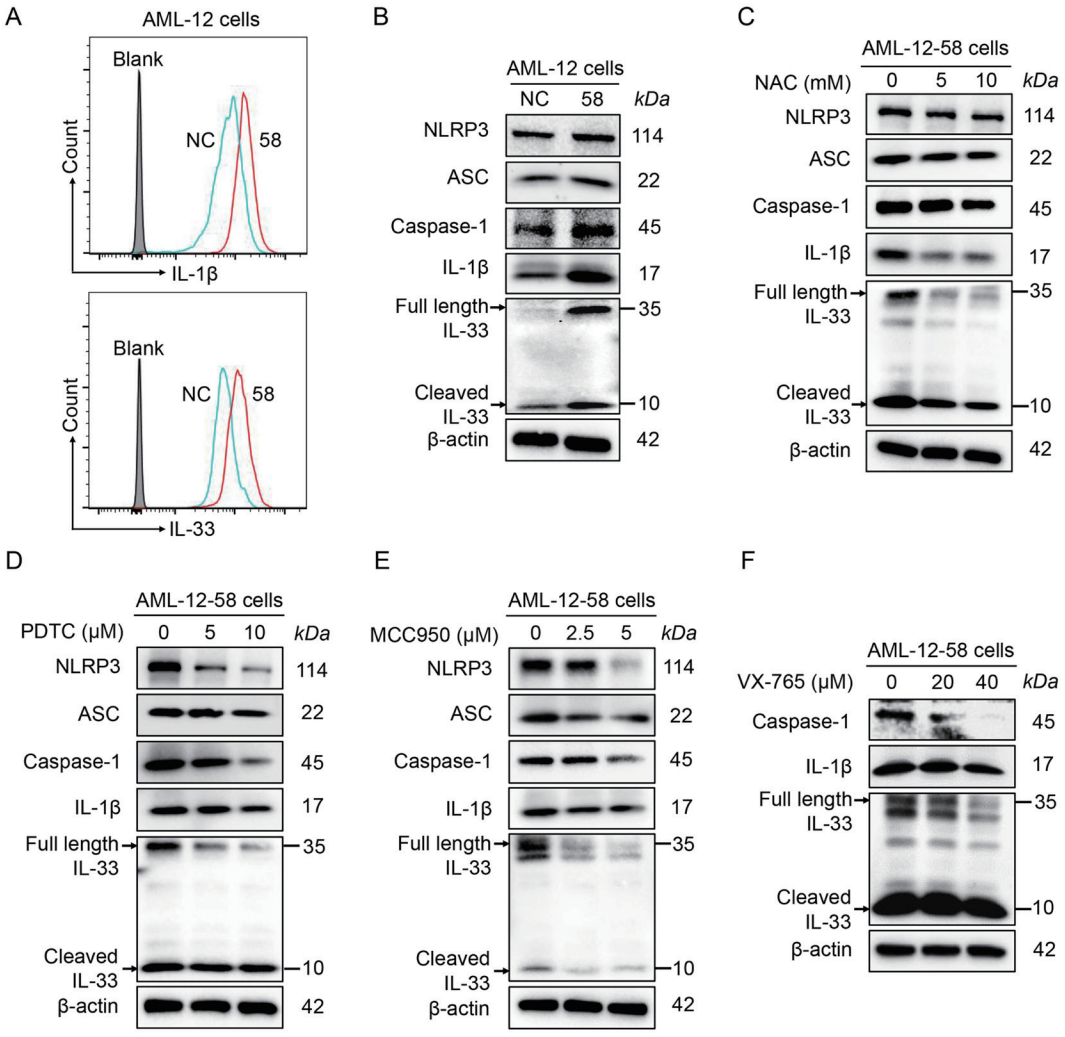

Fig. 6. GRIM19 (gene associated with retinoid-IFN-induced mortality 19) loss triggers aberrant NLRP3/IL33 activation through ROS/NF-κB signaling. (A) GRIM19 loss increases IL1β and IL33 levels. IL1β and IL33 cytokines were detected by flow cytometry in GRIM19-deficient AML12 cells. (B) GRIM19 loss triggers NLRP3 inflammasome activation *in vitro*. NLRP3 inflammasome complex, as well as IL1β and IL33, were detected by western blotting in GRIM19-deficient AML12 cells. (C) ROS inhibition attenuates GRIM19 loss-induced NLRP3 inflammasome activation *in vitro*. GRIM19-deficient AML12 cells were treated with NAC (0, 5, 10 mM) for 16 h. NLRP3 inflammasome, IL1β and IL33 were detected by western blotting. (D) NF-κB blockage decreases GRIM19 loss-triggered NLRP3 inflammasome activation *in vitro*. GRIM19-deficient AML12 cells were treated with NF-κB inhibitor PDTC (0, 5, 10 μM) for 16 h. NLRP3 inflammasome, IL1β, and IL33 levels were detected by western blotting. (E) NLRP3 inhibition reduces GRIM19 loss-induced IL1β and IL33 expression *in vitro*. GRIM19-deficient AMl12 cells were treated with NLRP3 inhibitor MCC950 (0, 2.5, 5 μM) for 16 h. NLRP3 inflammasome, IL1β, and IL33 were detected by western blotting. (F) Caspase1 repression attenuates GRIM19 loss-triggered IL1β and IL33 expression *in vitro*. GRIM19-deficient AML12 cells were treated with Caspase1 inhibitor VX765 (0, 20, 40 μM) for 24h. Caspase1, IL1β, and IL33 expressions were determined by western blotting. β-actin was used as a loading control. Data are presented as mean±SD of three independent experiments. Representative images are shown. IL, interleukin; NAC, N-acetylcysteine; PDTC, ammonium pyrrolidine dithiocarbamate; ASC, apoptosis-associated speck-like protein containing a caspase recruitment domain; NC, negative control.

complex in the processing of IL1β and IL33. As shown in Figure 6E, F, both MCC950 and VX765 treatment abrogated GRIM19 loss-driven IL1β and IL33 levels, indicating that the NLRP3 inflammasome exerts a pivotal role in GRIM19 loss-induced IL1β and IL33 expression in AML12 cells. Thus, these data indicate that GRIM19 loss contributes to abnormal NLRP3/IL33 activation through the ROS/NF-κB pathway.

Discussion

Deepening our understanding of the potential molecules involved in liver fibrogenesis would not only enhance our comprehension of HF pathogenesis but also identify promising approaches to treat or prevent liver fibrogenesis. Our previous study revealed a progressive decrease in GRIM19 protein during the progression of chronic atrophic gastritis, indicating a potential role for GRIM19 in digestive tract-related inflammation.[16–18] Although our preliminary data showed that GRIM19 inactivation promoted spontaneous hepatitis and liver fibrosis in mice,[19,20] the underlying mechanism remained largely unknown. Thus, it is crucial to understand whether and how GRIM19 loss contributes to liver fibrogenesis, particularly at the onset of hepatocyte injury, which is an initial event in chronic liver disease. Using human liver disease spectrum TMAs, we identified a progressive decrease in GRIM19 in chronic liver disease tissues ranging from hepatitis to cirrhosis to HCC. Following these findings, we generated a *GRIM19* KO mice model and *GRIM19*-deficient AML12

cells, revealing that hepatocyte-specific *GRIM19* knockout triggered spontaneous hepatitis followed by HF, caused by NLRP3/IL33 activation through ROS/NF-κB signaling. This study is the first to systematically elucidate the functional role of GRIM19 in liver fibrogenesis, offering a prospective diagnostic marker and therapeutic target for HF treatment.

As the most abundant cells in the liver, hepatocytes play a vital role in maintaining internal homeostasis and liver regeneration.[27] Although HSC activation has been well characterized during liver fibrogenesis in response to various inflammatory signals,[28–30] hepatocytes are considered the main target of most irritants, such as oxygen radicals, in various chronic liver diseases.[31] Thus, our investigation focused on potential targets responsible for hepatocyte damage observed during liver fibrogenesis. Mitochondria have recently received significant attention for their association with liver fibrogenesis. Oxidative stress induced by mitochondrial structural or functional disorders has been defined as one of the main causative agents of liver fibrosis.[11,13] mROS, a product of mitochondrial MRC I, significantly contributes to oxidative damage.[32,33] Mitochondrial GRIM19, a key subunit of mitochondrial MRC I, is considered essential for its normal functioning,[34] especially in maintaining mitochondrial activity.[35,36] Here, we have shown that GRIM19 loss led to oxidative DNA damage by inducing abnormal intracellular ROS and mROS *in vitro* and *in vivo*, resulting in decreased ATP content and GSH/GSSG ratios, as well as increased $NADP^+$/NADPH ratios in hepatocytes. These findings are further supported by a recent study on cardiac-specific *GRIM19* heterozygous deletion, where an ROS leak from complex I increased cytoplasm-localized H_2O_2.[34] Therefore, our data suggest that GRIM19 loss in hepatocytes is responsible for oxidative stress-induced liver injury, leading to liver fibrosis.

Our findings suggest that the NLRP3 inflammasome plays a crucial role in GRIM19 loss-induced liver fibrosis *in vivo*. Over the past several years, significant advances have been made in understanding the critical role of the NLRP3 inflammasome in HF.[23–25] Activation of the NLRP3 inflammasome can directly trigger chronic inflammation,[25] whereas NLRP3 inhibition can improve liver inflammation pathology and modulate the most critical outcome of liver fibrosis.[24] Importantly, the activated NLRP3 inflammasome can also activate resident KCs, which produce the inflammatory cytokine TNFα and profibrotic factor TGFβ1, resulting in HSC activation and liver fibrogenesis.[4,5,7,23–25] This is consistent with our observations in the two-year-old mice livers. The assembly of the inflammasome complex with ASC and caspase1 is mainly mediated by NLRP3 and facilitates the cleavage of proinflammatory cytokines such as IL1β and IL33.[37] mROS, as a secondary messenger in inflammatory signaling, plays a key role in the activation of the NLRP3 inflammasome through the NF-κB pathway.[38–40] We have found that GRIM19 loss induces chronic liver injury through ROS-mediated oxidative damage, resulting in aberrant NF-κB activation via an IKK/IκB partner. We have further revealed that GRIM19 loss induces abnormal NLRP3/IL33 activation through ROS/NF-κB signaling *in vivo* and *in vitro*, while pharmacological NLRP3 inhibition can attenuate GRIM19 loss-induced hepatitis and liver fibrosis in mice. Thus, our findings suggest that GRIM19 loss-triggered NLRP3/IL33 activation is responsible for HF pathogenesis, providing mechanistic insights into how GRIM19 loss drives liver fibrogenesis.

Our findings demonstrate NLRP3-dependent IL33 secretion and maturation during GRIM19 loss-induced liver fibrosis, offering promising prospects for clinical applications in the diagnosis and treatment of liver fibrosis. IL33, a member of the IL1 cytokine family, is considered an alarm hormone involved in immune regulation and the inflammatory response.[41] Clinical studies have revealed a significant accumulation of IL33 levels in the plasma of patients with chronic hepatitis, as well as in biopsy liver tissues of patients with HF and cirrhosis.[42,43] Additionally, increased IL33 levels can be detected in CCl_4-induced liver fibrosis in mice, while IL33 knockout significantly inhibited CCl_4 or cholestasis-induced HF progression.[43,44] Furthermore, IL33 derived from injured liver cells was shown to induce innate immune cells to produce TH2-type cytokines, promoting the polarization of M2 macrophages and further activating HSCs by releasing fibrotic factors such as TGFβ1.[45] Our study reveals that NLRP3 inhibition not only decreased GRIM19 loss-induced IL33 activation but also abrogated GRIM19 loss-driven liver fibrosis *in vivo*. Furthermore, we found that NLRP3 inhibition reduced GRIM19 loss-induced M2 macrophage aggregation, suggesting a crucial role for NLRP3/IL33 in GRIM19 loss-induced M2 macrophages during liver fibrosis. A recent study also identified NLRP3 as a critical transcription factor for IL33 in the epithelial cells of atopic dermatitis,[37] further indicating a crucial role for NLRP3-dependent IL33 activation in GRIM19 loss-driven liver fibrogenesis. Thus, our findings demonstrate NLRP3-dependent IL33 secretion and maturation during GRIM19 loss-induced liver fibrosis, providing a potential diagnostic target for clinical diagnosis of liver fibrosis and offering a promising therapeutic target for clinical treatment.

Our study presents a novel HF mouse model in which hepatocyte-specific *GRIM19* ablation can trigger spontaneous liver fibrosis, offering potential strategies for studying clinical interventions for liver fibrosis. Generally, genetic models rarely develop spontaneous liver fibrosis due to genetic manipulation and require restimulation to induce disease, except for MDR2-deficient mice, which develop biliary fibrosis.[46] Our study revealed that the genetic knockdown of *GRIM19* was sufficient to trigger spontaneous chronic liver fibrosis, providing potential clinical applications for preclinical drug assessment against liver fibrosis or therapeutic intervention of liver fibrosis through GRIM19 gene transfer. Intriguingly, our most recent study revealed a significant decrease in GRIM19 protein levels in CCl_4-treated fibrotic liver tissues, while adeno-associated virus 8 (AAV8)-mediated GRIM19 overexpression alleviated CCl_4-induced liver fibrogenesis by inhibiting NLRP3 activation,[47] indicating an essential role for GRIM19 activation in chemical-induced liver fibrosis. However, it remains unclear whether GRIM19 loss is also involved in diet-induced liver fibrosis, such as methionine- and choline-deficient, choline-deficient L-amino acid-defined, or high-fat high-sugar dietary animal models of nonalcoholic steatohepatitis, which are considered more suitable models to mimic pathophysiological progression than chemical CCl_4-induced liver fibrosis models.[48] Thus, further efforts are needed to investigate the role of GRIM19 loss in diet-related chronic liver diseases.

Our study has some limitations. First, although genomic hypermethylation was associated with GRIM19 downregulation,[17] the diverse and complex stimuli of liver injury make it challenging to understand the mechanism of GRIM19 loss in hepatocytes. Second, more long-term observations are needed to determine whether GRIM19 loss-driven liver fibrogenesis can progress into spontaneous HCC. Finally, we noted that hepatocyte-specific heterozygous *GRIM19*-deleted mice presented a lower birthrate compared to either *GRIM19* CKO or Alb-Cre mice (data not shown), indicating an essential role for GRIM19 in liver development in mice. Similar results can also be found in a recent report that complete *GRIM19* depletion was lethal for mouse embryos.[21,34] Thus, a tamoxifen-induced specific *GRIM19* knockout in hepatocytes should be

performed using Alb-Cre-ERT2 mice in the future. Mechanistically, previous reports showed a critical role of GRIM19 loss in autophagy in colorectal cancer and adenomyosis;[49,50] however, our unpublished data shows that neither apoptosis nor autophagy are involved in GRIM19 loss-induced liver fibrogenesis, suggesting that an unidentified mechanism contributes to GRIM19 loss-induced liver fibrogenesis.

Conclusion

Our research demonstrates that mitochondrial GRIM19 loss in hepatocytes triggers chronic liver fibrogenesis through NLRP3/IL33 activation via ROS/NF-κB signaling (Supplementary Fig. 8). This finding not only identifies a causal relationship between GRIM19 loss and liver fibrosis but also offers prospective therapeutic approaches for the treatment of liver fibrogenesis.

Acknowledgments

We thank Qixi Huang (Clayton High School, Clayton, Missouri, United States) for her writing assistance on the early version of this manuscript.

Funding

This study was partially supported by the National Nature Science Foundation of China [No.32171119; No.32371173]; the general basic research project from the Ministry of Education Key Laboratory of Child Development and Disorders [GBRP-202116]; the Nature Science Foundation of Chongqing Science and Technology Bureau [CSTB2022NSCQ-MSX0838]; the Science and Technology Research Program of Chongqing Municipal Education Commission [KJZD-K202100401]; and the Future Medical Youth Innovation Team Support Project of Chongqing Medical University [W0175].

Conflict of interest

The authors have no conflict of interests related to this publication.

Author contributions

Conception and design (XX, JF, YH), experiments and data analysis (XX, JF, XW, XZ, XH, YL, ZF, LZ, DH), article drafting (XX, JF, YH), critical article revision for important intellectual content (XX, MY, TL, LB, YH). All authors participated in the discussions and approved the manuscript.

Ethical statement

All procedures were reviewed and approved by the Institutional Animal Care and Use Committee of Chongqing Medical University (CHCMU-IACUC20210114023). All animals received humane care.

Data sharing statement

The data supporting the findings of this study are available in the supplementary material and the remaining data are available upon reasonable request from the corresponding author.

References

[1] Bray F, Ferlay J, Soerjomataram I, Siegel RL, Torre LA, Jemal A. Global cancer statistics 2018: GLOBOCAN estimates of incidence and mortality worldwide for 36 cancers in 185 countries. CA Cancer J Clin 2018;68(6):394–424. doi:10.3322/caac.21492, PMID:30207593.
[2] Cordero-Espinoza L, Huch M. The balancing act of the liver: tissue regeneration versus fibrosis. J Clin Invest 2018;128(1):85–96. doi:10.1172/JCI93562, PMID:29293095.
[3] Ginès P, Krag A, Abraldes JG, Solà E, Fabrellas N, Kamath PS. Liver cirrhosis. Lancet 2021;398(10308):1359–1376. doi:10.1016/S0140-6736(21)01374-X, PMID:34543610.
[4] Hammerich L, Tacke F. Hepatic inflammatory responses in liver fibrosis. Nat Rev Gastroenterol Hepatol 2023;20(10):633–646. doi:10.1038/s41575-023-00807-x, PMID:37400694.
[5] Gandhi CR. Hepatic stellate cell activation and pro-fibrogenic signals. J Hepatol 2017;67(5):1104–1105. doi:10.1016/j.jhep.2017.06.001, PMID:28939135.
[6] Antar SA, Ashour NA, Marawan ME, Al-Karmalawy AA. Fibrosis: Types, Effects, Markers, Mechanisms for Disease Progression, and Its Relation with Oxidative Stress, Immunity, and Inflammation. Int J Mol Sci 2023;24(4):4004. doi:10.3390/ijms24044004, PMID:36835428.
[7] Inzaugarat ME, Johnson CD, Holtmann TM, McGeough MD, Trautwein C, Papouchado BG, *et al*. NLR Family Pyrin Domain-Containing 3 Inflammasome Activation in Hepatic Stellate Cells Induces Liver Fibrosis in Mice. Hepatology 2019;69(2):845–859. doi:10.1002/hep.30252, PMID:30180270.
[8] Wang S, He L, Xiao F, Gao M, Wei H, Yang J, *et al*. Upregulation of GLT25D1 in Hepatic Stellate Cells Promotes Liver Fibrosis via the TGF-β1/SMAD3 Pathway In Vivo and In vitro. J Clin Transl Hepatol 2023;11(1):1–14. doi:10.14218/JCTH.2022.00005, PMID:36406310.
[9] Acharya P, Chouhan K, Weiskirchen S, Weiskirchen R. Cellular Mechanisms of Liver Fibrosis. Front Pharmacol 2021;12:671640. doi:10.3389/fphar.2021.671640, PMID:34025430.
[10] Schwabe RF, Tabas I, Pajvani UB. Mechanisms of Fibrosis Development in Nonalcoholic Steatohepatitis. Gastroenterology 2020;158(7):1913–1928. doi:10.1053/j.gastro.2019.11.311, PMID:32044315.
[11] Luangmonkong T, Suriguga S, Mutsaers HAM, Groothuis GMM, Olinga P, Boersema M. Targeting Oxidative Stress for the Treatment of Liver Fibrosis. Rev Physiol Biochem Pharmacol 2018;175:71–102. doi:10.1007/112_2018_10, PMID:29728869.
[12] Shojaie L, Iorga A, Dara L. Cell Death in Liver Diseases: A Review. Int J Mol Sci 2020;21(24):9682. doi:10.3390/ijms21249682, PMID:33353156.
[13] Mansouri A, Gattolliat CH, Asselah T. Mitochondrial Dysfunction and Signaling in Chronic Liver Diseases. Gastroenterology 2018;155(3):629–647. doi:10.1053/j.gastro.2018.06.083, PMID:30012333.
[14] Kisseleva T, Brenner D. Molecular and cellular mechanisms of liver fibrosis and its regression. Nat Rev Gastroenterol Hepatol 2021;18(3):151–166. doi:10.1038/s41575-020-00372-7, PMID:33128017.
[15] Nallar SC, Kalvakolanu DV. GRIM-19: A master regulator of cytokine induced tumor suppression, metastasis and energy metabolism. Cytokine Growth Factor Rev 2017;33:1–18. doi:10.1016/j.cytogfr.2016.09.001, PMID:27659873.
[16] Huang Y, Yang M, Hu H, Zhao X, Bao L, Huang D, *et al*. Mitochondrial GRIM-19 as a potential therapeutic target for STAT3-dependent carcinogenesis of gastric cancer. Oncotarget 2016;7(27):41404–41420. doi:10.18632/oncotarget.9167, PMID:27167343.
[17] Wang X, Ye T, Xue B, Yang M, Li R, Xu X, *et al*. Mitochondrial GRIM-19 deficiency facilitates gastric cancer metastasis through oncogenic ROS-NRF2-HO-1 axis via a NRF2-HO-1 loop. Gastric Cancer 2021;24(1):117–132. doi:10.1007/s10120-020-01111-2, PMID:32770429.
[18] Zeng X, Yang M, Ye T, Feng J, Xu X, Yang H, *et al*. Mitochondrial GRIM-19 loss in parietal cells promotes spasmolytic polypeptide-expressing metaplasia through NLR family pyrin domain-containing 3 (NLRP3)-mediated IL-33 activation via a reactive oxygen species (ROS) -NRF2- Heme oxygenase-1(HO-1)-NF-κB axis. Free Radic Biol Med 2023;202:46–61. doi:10.1016/j.freeradbiomed.2023.03.024, PMID:36990300.
[19] Xu X, Li R, Zeng X, Wang X, Xue B, Huang D, *et al*. [Pathogenic role of NDUFA13 inactivation in spontaneous hepatitis in mice and the mechanism]. Nan Fang Yi Ke Da Xue Xue Bao 2021;41(1):55–63. doi:10.12122/j.issn.1673-4254.2021.01.07, PMID:33509753.
[20] Xu X, Zeng X, Li R, Feng J, Huang D, Huang Y. [Mechanism of hepatocyte mitochondrial NDUFA13 deficiency-induced liver fibrogenesis: the role of abnormal hepatic stellate cell activation]. Nan Fang Yi Ke Da Xue Xue Bao 2021;41(4):529–535. doi:10.12122/j.issn.1673-4254.2021.04.07, PMID:33963711.
[21] Kalakonda S, Nallar SC, Jaber S, Keay SK, Rorke E, Munivenkatappa R, *et al*. Monoallelic loss of tumor suppressor GRIM-19 promotes tumorigenesis in mice. Proc Natl Acad Sci U S A 2013;110(45):E4213–E4222. doi:10.1073/pnas.1303760110, PMID:24145455.
[22] Luedde T, Schwabe RF. NF-κB in the liver—linking injury, fibrosis and hepatocellular carcinoma. Nat Rev Gastroenterol Hepatol 2011;8(2):108–118. doi:10.1038/nrgastro.2010.213, PMID:21293511.
[23] Zhou R, Yazdi AS, Menu P, Tschopp J. A role for mitochondria in NLRP3 inflammasome activation. Nature 2011;469(7329):221–225. doi:10.1038/nature09663, PMID:21124315.
[24] Mridha AR, Wree A, Robertson AAB, Yeh MM, Johnson CD, Van Rooyen DM, *et al*. NLRP3 inflammasome blockade reduces liver inflammation and fibrosis in experimental NASH in mice. J Hepatol 2017;66(5):1037–1046. doi:10.1016/j.jhep.2017.01.022, PMID:28167322.
[25] de Carvalho Ribeiro M, Szabo G. Role of the Inflammasome in Liver Disease. Annu Rev Pathol 2022;17:345–365. doi:10.1146/annurev-pathmechdis-032521-102529, PMID:34752711.
[26] Tan Z, Liu Q, Jiang R, Lv L, Shoto SS, Maillet I, *et al*. Interleukin-33 drives hepatic fibrosis through activation of hepatic stellate cells. Cell Mol Immu-

nol 2018;15(4):388–398. doi:10.1038/cmi.2016.63, PMID:28194023.
[27] Malato Y, Naqvi S, Schürmann N, Ng R, Wang B, Zape J, *et al*. Fate tracing of mature hepatocytes in mouse liver homeostasis and regeneration. J Clin Invest 2011;121(12):4850–4860. doi:10.1172/JCI59261, PMID:22105172.
[28] Hellerbrand C, Stefanovic B, Giordano F, Burchardt ER, Brenner DA. The role of TGFbeta1 in initiating hepatic stellate cell activation in vivo. J Hepatol 1999;30(1):77–87. doi:10.1016/s0168-8278(99)80010-5, PMID: 9927153.
[29] Schmitt-Gräff A, Krüger S, Bochard F, Gabbiani G, Denk H. Modulation of alpha smooth muscle actin and desmin expression in perisinusoidal cells of normal and diseased human livers. Am J Pathol 1991;138(5):1233–1242. PMID:2024709.
[30] Bourebaba N, Marycz K. Hepatic stellate cells role in the course of metabolic disorders development - A molecular overview. Pharmacol Res 2021;170:105739. doi:10.1016/j.phrs.2021.105739, PMID:34171492.
[31] Higuchi H, Gores GJ. Mechanisms of liver injury: an overview. Curr Mol Med 2003;3(6):483–490. doi:10.2174/1566524033479528, PMID:14527080.
[32] Schieber M, Chandel NS. ROS function in redox signaling and oxidative stress. Curr Biol 2014;24(10):R453–R462. doi:10.1016/j.cub.2014.03.034, PMID:24845678.
[33] Zuo L, Zhou T, Pannell BK, Ziegler AC, Best TM. Biological and physiological role of reactive oxygen species—the good, the bad and the ugly. Acta Physiol (Oxf) 2015;214(3):329–348. doi:10.1111/apha.12515, PMID:25912260.
[34] Hu H, Nan J, Sun Y, Zhu D, Xiao C, Wang Y, *et al*. Electron leak from NDUFA13 within mitochondrial complex I attenuates ischemia-reperfusion injury via dimerized STAT3. Proc Natl Acad Sci U S A 2017;114(45):11908–11913. doi:10.1073/pnas.1704723114, PMID:29078279.
[35] Lu H, Cao X. GRIM-19 is essential for maintenance of mitochondrial membrane potential. Mol Biol Cell 2008;19(5):1893–1902. doi:10.1091/mbc.e07-07-0683, PMID:18287540.
[36] Angebault C, Charif M, Guegen N, Piro-Megy C, Mousson de Camaret B, Procaccio V, *et al*. Mutation in NDUFA13/GRIM19 leads to early onset hypotonia, dyskinesia and sensorial deficiencies, and mitochondrial complex I instability. Hum Mol Genet 2015;24(14):3948–3955. doi:10.1093/hmg/ddv133, PMID:25901006.
[37] Zheng J, Yao L, Zhou Y, Gu X, Wang C, Bao K, *et al*. A novel function of NLRP3 independent of inflammasome as a key transcription factor of IL-33 in epithelial cells of atopic dermatitis. Cell Death Dis 2021;12(10):871. doi:10.1038/s41419-021-04159-9, PMID:34561424.
[38] Hernández-Alvarez MI, Sebastián D, Vives S, Ivanova S, Bartoccioni P, Kakimoto P, *et al*. Deficient Endoplasmic Reticulum-Mitochondrial Phosphatidylserine Transfer Causes Liver Disease. Cell 2019;177(4):881–895.e17. doi:10.1016/j.cell.2019.04.010, PMID:31051106.
[39] Zhong Z, Umemura A, Sanchez-Lopez E, Liang S, Shalapour S, Wong J, *et al*. NF-κB Restricts Inflammasome Activation via Elimination of Damaged Mitochondria. Cell 2016;164(5):896–910. doi:10.1016/j.cell.2015.12.057, PMID:26919428.
[40] Afonina IS, Zhong Z, Karin M, Beyaert R. Limiting inflammation-the negative regulation of NF-κB and the NLRP3 inflammasome. Nat Immunol 2017;18(8):861–869. doi:10.1038/ni.3772, PMID:28722711.
[41] Kotsiou OS, Gourgoulianis KI, Zarogiannis SG. IL-33/ST2 Axis in Organ Fibrosis. Front Immunol 2018;9:2432. doi:10.3389/fimmu.2018.02432, PMID:30405626.
[42] Gao Y, Liu Y, Yang M, Guo X, Zhang M, Li H, *et al*. IL-33 treatment attenuated diet-induced hepatic steatosis but aggravated hepatic fibrosis. Oncotarget 2016;7(23):33649–33661. doi:10.18632/oncotarget.9259, PMID:27172901.
[43] Mehraj V, Ponte R, Routy JP. The Dynamic Role of the IL-33/ST2 Axis in Chronic Viral-infections: Alarming and Adjuvanting the Immune Response. EBioMedicine 2016;9:37–44. doi:10.1016/j.ebiom.2016.06.047, PMID:27397514.
[44] McHedlidze T, Waldner M, Zopf S, Walker J, Rankin AL, Schuchmann M, *et al*. Interleukin-33-dependent innate lymphoid cells mediate hepatic fibrosis. Immunity 2013;39(2):357–371. doi:10.1016/j.immuni.2013.07.018, PMID:23954132.
[45] Cayrol C, Girard JP. Interleukin-33 (IL-33): A nuclear cytokine from the IL-1 family. Immunol Rev 2018;281(1):154–168. doi:10.1111/imr.12619, PMID:29247993.
[46] Fickert P, Zollner G, Fuchsbichler A, Stumptner C, Weiglein AH, Lammert F, *et al*. Ursodeoxycholic acid aggravates bile infarcts in bile duct-ligated and Mdr2 knockout mice via disruption of cholangioles. Gastroenterology 2002;123(4):1238–1251. doi:10.1053/gast.2002.35948, PMID:12360485.
[47] Xu X, Feng J, Luo Y, He X, Zang J, Huang D. [Adeno-associated virus-mediated hepatocyte-specific NDUFA13 overexpression protects against CCl(4)-induced liver fibrosis in mice by inhibiting hepatic NLRP3 activation]. Nan Fang Yi Ke Da Xue Xue Bao 2024;44(2):201–209. doi:10.12122/j.issn.1673-4254.2024.02.01, PMID:38501404.
[48] Ibrahim SH, Hirsova P, Malhi H, Gores GJ. Animal Models of Nonalcoholic Steatohepatitis: Eat, Delete, and Inflame. Dig Dis Sci 2016;61(5):1325–1336. doi:10.1007/s10620-015-3977-1, PMID:26626909.
[49] Zhang J, Chu D, Kawamura T, Tanaka K, He S. GRIM-19 repressed hypoxia-induced invasion and EMT of colorectal cancer by repressing autophagy through inactivation of STAT3/HIF-1α signaling axis. J Cell Physiol 2019;234(8):12800–12808. doi:10.1002/jcp.27914, PMID:30537081.
[50] Huang Y, Zhao Y, Liu H, Yang Y, Cheng L, Deng X, *et al*. Decreased expression of GRIM-19 induces autophagy through the AMPK/ULK1 signaling pathway during adenomyosis†. Biol Reprod 2022;107(4):956–966. doi:10.1093/biolre/ioac151, PMID:35908189.